Original Research

Effects of *Rosmarinus officinalis* extract on human primary omental preadipocytes and adipocytes

Bruno Stefanon, Elena Pomari and Monica Colitti

Department of Agricultural and Environmental Sciences, University of Udine, 33100 Udine, Italy
Corresponding author: Monica Colitti. Email: monica.colitti@uniud.it

Abstract

The prevalence of obesity is increasing all over the world. Although it has been shown that natural substances influence fat metabolism, little is known about the effect on cellular and molecular mechanisms in human. In this *in vitro* study, the activity of *Rosmarinus officinalis* (RO) standardized extract in modulating human primary visceral preadipocytes differentiation, lipolysis, and apoptosis was investigated. Moreover, gene expression of key adipogenesis modulators and microRNAs-seq were evaluated. Preadipocytes treated with RO extract significantly reduced triglyceride incorporation during maturation in a dose-dependent manner without affecting cell viability. In addition, RO extract stimulated lipolytic activity in differentiating preadipocytes and mature adipocytes in treated cells compared to controls. Differentiating preadipocytes incubated in the presence of RO extract showed a decreased expression of cell cycle genes such as cyclin D1, cyclin-dependent kinase 4, cyclin-dependent kinase inhibitor 1A (p21, Cip1) and an increased expression of GATA binding protein 3, wingless-type MMTV integration site family, member 3A mRNA levels. Recent studies have demonstrated that some phytochemicals alter the expression of specific genes and microRNAs that play a fundamental role in the pathogenesis of obesity and related diseases. Interestingly, genes modulated in RO-treated cells were found to be validated miRNAs targets, such as let-7f-1, miR-17, and miR-143. The results indicated that RO extract modulates human adipocyte differentiation and significantly interferes with adipogenesis and lipid metabolism, supporting its interest as dietary supplement.

Keywords: Human visceral adipocytes, differentiation, gene expression, microRNA, *Rosmarinus officinalis*

***Experimental Biology and Medicine* 2015; 240: 884–895. DOI: 10.1177/1535370214562341**

Introduction

Human obesity is a serious health problem all over the world in both developed and developing countries.[1,2] Obesity is the result of a positive energy balance, where the adipose tissue is the primary site for energy storage. It is also well established that the adipose tissue is an endocrine organ responsible for the secretion of numerous adipokines that overall play a key role not only in the control of energy balance, but also in the maintenance of the metabolic homeostasis.[3,4] Increased metabolic disorders and diseases, such as type-2 diabetes, dyslipidemia, hypertension, and cardiovascular diseases are associated with obesity.[5–7] At cellular level, obesity is characterized by hypertrophy (cell size increase) and hyperplasia (cell number increase) of adipocytes, processes that are largely dependent on the regulation of adipocyte differentiation.[8]

Therapies against obesity, based on lifestyle modifications and pharmacological drugs, have failed to provide lasting weight loss in obese and overweight people.[9] At this regard, the potential treatments against obesity would target adipocytes, the formation of new mature adipocytes from undifferentiated precursors, and their molecular pathways.[10] Evidences suggest that the phytochemical constituents of natural extracts may exert antiobesity effects by inhibiting adipogenesis and attenuating the growth of adipose tissue by inducing apoptosis and promoting lipolysis of mature adipocytes.[11–14]

Rosmarinus officinalis (RO) is a woody, perennial herb native to the Mediterranean region. A number of studies have reported its therapeutic potentials as antioxidant, hepatoprotective, anti-inflammatory, and antimicrobial activity.[15–17] The main components present in RO are phenolic diterpenes (carnosic acid, carnosol, rosmadial, rosmanol), flavonoids phenolic acids, and essential oils.

Recent reports showed that a rosemary leaf extract limits weight gain and liver steatosis in mice fed with a high-fat diet.[18] It has been also reported that carnosic acid, the

main bioactive compound of RO extract, inhibits 3T3-L1 preadipocytes differentiation by activation of the antioxidant response element and induction of phase II enzymes involved in the metabolism of glutathione (GSH), leading to an increase of the intracellular level of GSH.[19]

Only recently, the molecular mechanism responsible for its antiadipogenic effect has been elucidated. Carnosic acid has been demonstrated to decrease lipid accumulation and to inhibit differentiation of 3T3-L1 preadipocyte. Carnosic acid alters mitotic clonal expansion (MCE) and the ratio of the different C/EBP forms, induces the loss of C/EBPβ proper subnuclear distribution, and inhibits the expression of C/EBPα and PPARγ.[20] Moreover, carnosic acid reduces lipid absorption in the gut of olive oil-loaded mice inhibiting the pancreatic lipase, therefore decreases body weight *in vivo*.[21]

The molecular events that take place during the process of adipogenesis have been extensively studied on 3T3-L1, the mouse embryonic fibroblast cell line, since these cells have the ability to differentiate into cells that accumulate lipids, respond to insulin, and secrete leptin.[22,23] In the 3T3-L1, the cascades of genetic and signaling events that take place during adipocyte differentiation are well characterized.[24–26]

Recent studies have been demonstrated that some phytochemicals, such as resveratrol,[27] curcumin,[28] and epigallocatechin-3-gallate (EGCG),[29] regulate microRNAs (miRNAs) and downstream the related target genes.

miRNAs are large class of short non-coding RNAs (~22–24 nt) that regulate a variety of biological processes at the post-transcriptional level by controlling mRNA stability, translation, or degradation. Since miRNAs are mechanisms of gene regulation in both normal and diseased conditions, recent findings suggest an emerging role of miRNAs as gene transcriptional regulation tool and possible drug development.[30] During adipogenesis, miRNAs can accelerate or inhibit adipocyte differentiation and therefore they modulate cell fate.[30–32] It has been shown that miRNAs are involved in the pathological development of obesity by affecting adipocyte differentiation and lipid metabolism; their expression is dependent upon the developmental stage and the pathological condition of the cell, i.e. obese or lean.[33] It has been shown that patients treated with thiazolidinediones, a PPARγ agonist, displayed different miRNAs expression profiling in subcutaneous and visceral fat tissue.[34] Moreover, fisetin[35] and green tea[36] have been shown to alter the expression of specific genes and miRNAs involved in the pathogenesis of obesity and related diseases.

The goal of this work was to analyze the modulation of cellular activity and of genes involved in the adipogenesis pathway on primary human omental preadipocytes and mature adipocytes. In particular, the effects of RO extract were tested *in vitro* on cell viability, apoptosis, lipolysis, and adipogenesis in preadipocytes at 20 days of differentiation. In addition, expression levels of genes involved in human adipogenesis pathway, investigated by PCR array, and the modulation of miRNAs by miRNAs-seq were also evaluated.

Materials and methods

Plant extract

RO extract was provided from company ACEF S.p.a. (Piacenza, Italy). The dried extract was obtained from leaf and contained ≥20% phenolic diterpenes and ≥10% carnosic acid. The extract (50 mg) was dissolved in 1 mL of 10% dimethylsulfoxide (DMSO), filtered with 0.22 μm pore size (Millipore, Milan, Italy) and kept in the dark at −20°C until further analysis.

Cell culture and cell treatment

Cells and media were obtained from Zen-Bio (USA). Primary omental preadipocytes were collected from Caucasian normal (non-diabetic and non-smoker) women donors ($n = 3$). The mean donor age was 48.67 ± 9.07 years and mean BMI was $42.70 \pm 6.95\ kg/m^2$. Preadipocytes were cultured in omental preadipocytes medium (OM-PM). In order to differentiate preadipocytes into adipocytes, omental differentiation medium (OM-DM) was used. Differentiated adipocytes were cultured in omental adipocyte maintenance medium (OM-AM). All cells were maintained in humidified air with 5% CO_2 at 37°C.

Cells (passage 3) were treated with RO extract at increasing concentrations and during different stage of differentiation with the same final concentration of 0.014% DMSO in the culture medium. The control cells (CTRL) were incubated with the same final amount of 0.014% DMSO in culture medium. Treatments were performed in three different stages of the cell life cycle: (1) on preadipocytes for eight days (P8) in OM-PM; (2) on preadipocytes for 10 days (P10) and 20 days (P20) during differentiation in OM-DM; and (3) on mature fully differentiated adipocytes for seven days (A7) in OM-AM.

For the apoptosis, lipolysis, and adipogenesis assays, cells were seeded in a 96-well plate at a density of 10^4 cell/well. For PCR assay, cells were seeded in a six-well plate at a density of 1×10^5 cell/well and left to grow overnight.

All analyses were performed using cells of the three different donors and each donor was assayed in triplicates.

Cell viability

The influence of the RO extract at different concentrations (5, 10, 30, and 70 μg/mL) on cellular viability was determined by the 3-(4,5-dimethylthiazol-2-yl)-2,5-diphenyltetrazolium bromide (MTT) colorimetric assay.[37] For the assay, cells were seeded in a 96-well plate at a density of 10^4 cells/well. Cell viability was measured on P8, P10, P20, and A7 cells. Cells were then washed with phosphate buffered saline (PBS) and 20 μL of MTT reagent (Sigma, Milano, Italy) was added to each well, and the plates were incubated for 3 h at 37°C. Next, the mixture in each well was removed, and formazan crystals formed were dissolved in 100 μL of DMSO. Absorbance was read at 570 nm with a microplate reader, and the surviving cell fraction was calculated. The cell viability was expressed as a percentage relative to CTRL cells.

Apoptosis assay

In order to detect apoptosis, ApoStrand™ ELISA apoptosis detection kit (Enzo Life Sciences Inc., NY, USA) was used according to provider's instructions. This assay is based on the denaturation of DNA in apoptotic cells by formamide, which reproduces changes in chromatin related to apoptosis. The denatured DNA is revealed with a mixture of primary antibody and peroxidase-labeled secondary antibody. P8, P20, and A7 RO-treated cells (30 μg/mL) were fixed for 30 min and dried in an oven at 56°C for 20 min. Subsequently, cells were incubated with formamide at 56°C for 30 min. Then, blocking solution was added and cells were incubated with antibody mixture for 30 min. After washing with 1X wash buffer, cells were incubated with 100 mL of peroxidase substrate and absorbance was read using an ELISA plate reader at 405 nm. The apoptotic positive control (single-stranded DNA in PBS) was also included in the analysis.

Lipolysis assay

Lipolytic activity was detected with AdipoLyze™ Lipolysis Detection Kit (Lonza Walkersville Inc., MD, USA) according to provider's instructions. The assay is a fluorescent kit designed to quantify the glycerol released by cells undergoing lipolysis. The glycerol detection was performed on P20 and A7 cells. An amount of 50 μL of the culture medium supplemented with RO extract was removed from each well and added to a new 96-well plate. Fifty microliters of enzyme/detection solution was added in each well. Afterward, 1 h of incubation in dark was performed. Finally, fluorescence was read at 570 nm excitation and 595 nm emission wavelength with a fluorescent microplate reader. Orbital shaking for 5 s was applied before measurement. Data were compared with a standard curve of fluorescence obtained from measurements of standard glycerol from 0.0 to 108.6 μM.

Oil Red O staining and measurement of lipid accumulation

In order to quantify lipid accumulation, Oil-Red O staining (Sigma, Milan, Italy) was used. The assay was performed on treated and CTRL P10 and P20 cells. After RO extract (30 μg/mL) treatment on 96-well culture plate, cells were first rinsed with PBS and then fixed with 4% formaldehyde for 30 min. Cells were stained with the ORO working solution (40% of Oil-Red O staining and 60% of milliQ water) for 20 min at 25°C and examined by an optical microscope (PrimoVert, Zeiss, Jena Germany) to evaluate lipid accumulation. Lipids were extracted from the cells using DMSO and quantified with a microplate reader at 510 nm. Data were expressed as percentage of lipid accumulation versus CTRL.

RNA extraction and adipogenesis PCR array

Treated and CTRL P20 cells were washed with cold PBS before total RNA extraction using miRNeasy kit with QIAzol Lysis Reagent (Qiagen, Milan, Italy), according to the manufacturer's instructions to get two elutions: small RNAs and larger RNAs. To perform PCR array, the cDNA was synthesized from the purified larger RNA samples according to RT^2 First Strand kit (Qiagen, Milan, Italy). Briefly, the 10 μL of Genomic DNA Elimination Mixture including 1 μg of the purified RNA was incubated at 42°C for 5 min. Then, mixture was immediately placed on ice for 1 min and added with 20 μL of RT reaction mixture. Tubes were incubated at 42°C for 15 min and at 95°C for 5 min. Afterward, 91 μL of RNase-free H_2O were added to each 30 μL of cDNA synthesis reaction.

The expression profile of adipogenesis was performed using ready-to-use human Adipogenesis RT^2 Profiler PCR Array (PAHS-049 Z; Qiagen, Milan, Italy) containing primers for 84 tested, five housekeeping genes and controls for RT and PCR reactions. The cDNA synthesized was used for preparation of reaction mixture accordingly instructions of RT^2 SYBR® Green qPCR Mastermix kit (Qiagen, Milan, Italy). To each of 96-well plate, 20 μL reaction mixture based on CFX96 Real-Time PCR Detection System (Bio-Rad, Milano, Italy) was added. Thermal cycling recommended by plates manufacturer for Bio-Rad CFX96 was used (10 min initial denaturation at 95°C followed by 40 cycles: 15 s at 95°C, 30 s amplification at 55°C, and 30 s extension at 72°C). Calculations of contamination with human genomic DNA accordingly to manufacturer's instructions showed lack of contamination on all plates. Beta-2-microglobulin (B2M), glyceraldehyde-3-phosphate dehydrogenase (GAPDH), hypoxanthine phosphoribosyltransferase 1 (HPRT1), and ribosomal protein L13a (RPL13A) were chosen from the group of five housekeeping genes as the best and least varying reference genes. Beta-actin (ACTB) was not used, since the coefficient of variation of the Ct values was more than twofold than that of other housekeeping genes. The expression of target genes was normalized and ΔCts were calculated by the difference between Ct of target genes and the geometric mean of the four housekeeping genes. Differences between RO samples and controls were calculated using the $2^{-\Delta\Delta Ct}$ method,[38,39] where $2^{-\Delta\Delta Ct}$ represents the difference of a given target gene in treated cells versus CTRL. The *n*-fold expression of a given target gene was calculated as $\log_2(2^{-\Delta\Delta Ct})$.

miRNA-seq analysis

The effects of RO extract on expression pattern of miRNAs was investigated on P20 cells ($n = 3$) without (CTRL) or treated with 30 μg/mL RO extract.

The small RNA samples purified (see paragraph earlier) were processed into sequencing libraries using Illumina HiSeq2000 platform (http://www.illumina.com/systems/genome_analyzer) for a miRNA sequencing output of 10M reads/sample. For bioinformatic analysis, raw sequences were trimmed to remove adapter sequence and the resulted unique tags were counted. Each unique sequence (tag) was aligned to identify read correspondences to RNA and a table of counts for each RNA in each sample was generated. Count-based differential expression analysis and normalization of RNAseq data[40] were performed using

Table 1 Modulation by RO extract of MTT metabolism in human omental preadipocytes. Cells were treated with 30 μg/mL RO extract

Dose (μg/mL)	P8	P10	P20	A7
5	$89.62^{A} \pm 0.65$	$92.56^{A} \pm 2.72$	$90.80^{A} \pm 1.10$	$96.78^{A} \pm 0.71$
10	$78.52^{B} \pm 0.46$	$74.14^{B} \pm 2.70$	$78.48^{B} \pm 0.87$	$95.54^{A} \pm 0.67$
30	$67.94^{C} \pm 0.77$	$73.03^{B} \pm 3.17$	$69.22^{C} \pm 0.79$	$93.88^{A} \pm 0.69$
70	$32.94^{D} \pm 1.77$	$53.59^{C} \pm 3.83$	$45.12^{D} \pm 0.74$	$89.69^{B} \pm 0.63$

P8, preadipocytes treated for eight days; P10 differentiating preadipocytes treated for 10 days; P20 differentiating preadipocytes treated for 20 days; A7, mature adipocytes treated for seven days. Data are mean ± SEM. Different superscript capital letters indicate significant differences ($P < 0.001$) within treatments at different concentrations.

edgeR software.[41] The results were presented as number of transcripts.

Search of target genes of miRNAs

miRWalk web tool was then used to search the gene targets of miRNAs.[42] Significantly ($P < 0.05$ and $P < 0.001$) up and down-regulated miRNAs obtained by miRNA-seq were imported into miRWalk and only the validated gene targets were acquired. Moreover, miRNAs-adipocyte, downloaded from miRWalk database, were used to identify their associated gene targets. The VENNY tool[43] was thus used to compare the validated genes obtained from the aforementioned analyses with the significantly ($P < 0.05$) regulated genes detected by PCR array.

The list of validated target genes from differentially expressed miRNAs of RO-treated P20 cells, obtained by miRWalk web tool, and then the shared genes, obtained by Venny diagram, were uploaded in Database for Annotation, Visualization and Integrated Discovery (DAVID version 6.7) to provide an enrichment analysis of common genes with all known gene ontology (GO) term analysis and Kyoto Encyclopedia of Genes and Genomes (KEGG) pathways.[44]

Statistical analysis

Data were analyzed with ANOVA (SPSSx, 2007). For cell viability analysis, the model included the amount of RO as fixed effect (four doses; 36 observations). For apoptosis, the model included the fixed effect of treatment (RO and CTRL, two levels) and times of incubation (three levels, P8, P20, and A7; 54 observations). For the triglyceride accumulation assay, the model included the fixed effect of treatment (RO and CTRL, two levels) and times of incubation (two levels, P10 and P20; 36 observations). For lipolysis assay, the model included the fixed effect of treatment (RO and CTRL, two levels) and times of incubation (two levels, P20 and A7; 36 observations). miRNAs data were analyzed with T-test. PCR array data, expressed as $\log_2(n\text{-fold})$, were analyzed using one-sample t-test.[45] For a graphical appraisal and to quickly identify changes in PCR array $\log_2(n\text{-fold})$, Volcano plot was used and the statistical significance was reported at $P < 0.05$, as −Log(p value).

Results

Cell viability

A viability assay was used to investigate potential negative effects of RO extract. P8, P10, P20, and A7 cells were treated with 5, 10, 30, or 70 μg/mL. In particular, the analysis showed that cell viability on P8, P10, and P20 cells treated with RO extract significantly ($P < 0.001$) decreased in a dose-dependent manner (Table 1), and the 70 μg/mL dose was always significantly different from other doses. Nevertheless, viability remained over 60% up to 30 μg/mL dose and markedly decrease at 70 μg/mL; only in A7 cells remained over 80% up to 70 μg/mL dose.

From these evidences, 30 μg/mL of plant extract was chosen for the further experiments.

Effect of RO on apoptosis

The apoptotic effect was examined on P8, P20, and A7 cells treated with 30 μg/mL RO extract and on corresponding CTRL cells. A significant ($P < 0.001$) apoptotic activity of RO on P8 and P20 cells was observed (Figure 1). On the contrary, RO did not show any change of apoptotic activity on A7 cells compared to CTRL cells. The interaction between cells at different stages and treatments was also significantly different ($P < 0.001$). The apoptotic positive control was 2.47 ± 0.02 of absorbance unit.

RO extract decreases triglyceride accumulation

The effects of RO extract on triglyceride accumulation was investigated on P10 and P20 cells treated with 30 μg/mL RO extract and on the corresponding CTRL cells. The total amount of lipid accumulation was reported as percentage respect to CTRL (as 100%) (Figure 2(a)). P10 and P20 exhibited significant ($P < 0.001$) decreased triglyceride levels compared to CTRL.

In agreement with these results, the majority of CTRL cells presented triglycerides (Oil red staining) in the lipid droplets (Figure 2(b)). In contrast, cells incubated with RO extract did not appear to accumulate lipid droplets, as observed from the absence of red staining. The revealed few vesicles were smaller in size with respect to those in CTRL cells.

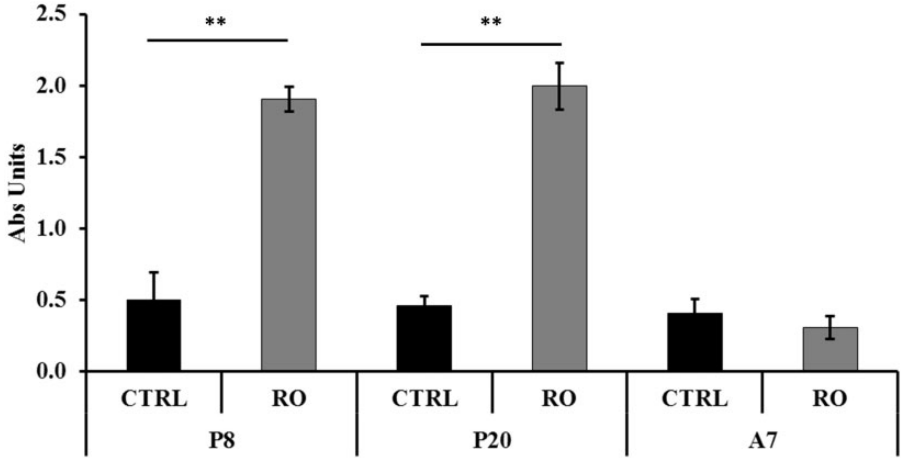

Figure 1 Modulation by RO extract of apoptosis in human omental preadipocytes. Cells were treated with 30 μg/mL RO extract. P8, preadipoctes treated for eight days; P20, differentiating preadipocytes treated for 20 days; A7, mature adipocytes treated for seven days. Data are mean ± standard error of the mean (SEM). Asterisks indicate the significant difference between treatments for $P < 0.001$. Results are given in absorbance units (Abs units).

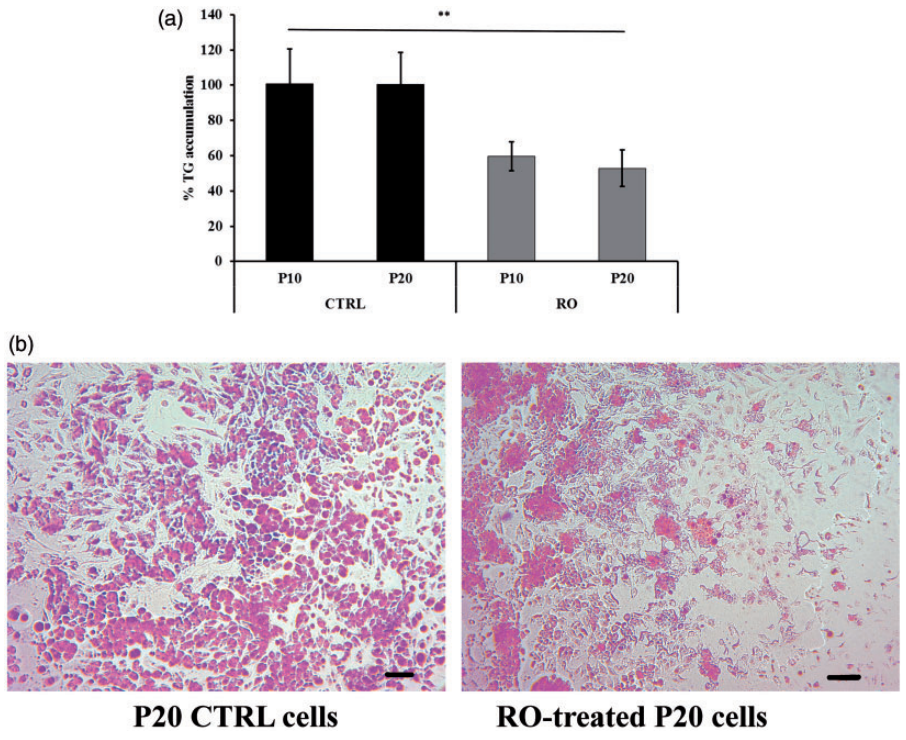

Figure 2 Effects of RO extract on triglyceride accumulation during preadipocyte differentiation. P20, differentiating preadipocytes treated for 20 days; A7, mature adipocytes treated for seven days. (a) Triglyceride accumulation of differentiating preadipocytes incubated 20 days (P20) with RO extract relative to untreated control cells (CTRL) set as 100%. Results are depicted as mean ± standard error of the mean (SEM). Asterisks indicate the significant difference between treatments for $P < 0.001$. (b) Images after triglyceride Oil red O staining from P20 cell populations with and without 30 μg/mL RO extract and P20 untreated control cells (CTRL). Scale bar: 200 μm. Cells were used at the third passage. (A color version of this figure is available in the online journal.)

RO extract increases glycerol release

The lipolysis activity was assessed on P20 and A7 cells treated with 30 μg/mL RO extract and on the corresponding CTRL cells. Treatment of P20 cells with RO extract significantly ($P < 0.001$) incremented the content of free glycerol to 122.9 μM (±11.2) as compared to 93.2 μM (±4.1) in CTRL cells. Treatment of A7 cells with RO extract significantly ($P < 0.001$) incremented the content of free glycerol to 94.7 μM (±13.4) as compared to 2.5 μM (±0.6) in CTRL cells (Figure 3).

Effects of RO extract on the gene expression of adipogenesis-associated genes

The expression pattern of genes involved in the adipogenesis pathways was further profiled using a PCR array. Volcano plot showed significantly ($P < 0.05$) up- and down-regulated genes in comparison to CTRL cells (Figure 4). In particular, the expression of cell cycle genes cyclin-dependent kinase 4 (CDK4), cyclin D1 (CCND1), and cyclin-dependent kinase inhibitor 1A (p21, Cip1) (CDKN1A) significantly decreased ($P < 0.05$); CEBPα,

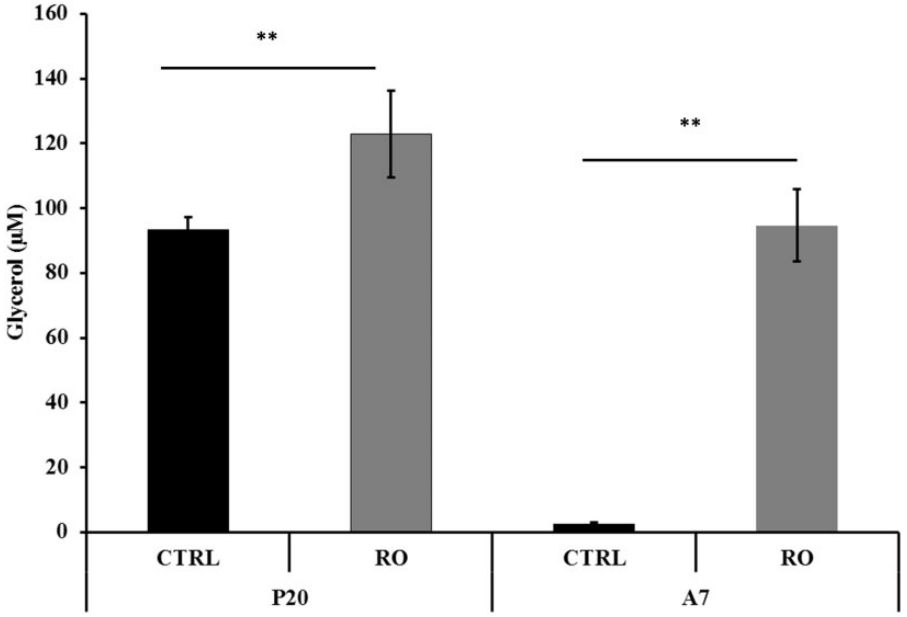

Figure 3 Determination of glycerol release in differentiating (P20) and mature (A7) adipocytes after incubation with RO extract solution. Glycerol content is given in μM. Results are depicted as mean ± standard error of the mean (SEM). Asterisks indicate the significant difference between treatments for $P < 0.001$

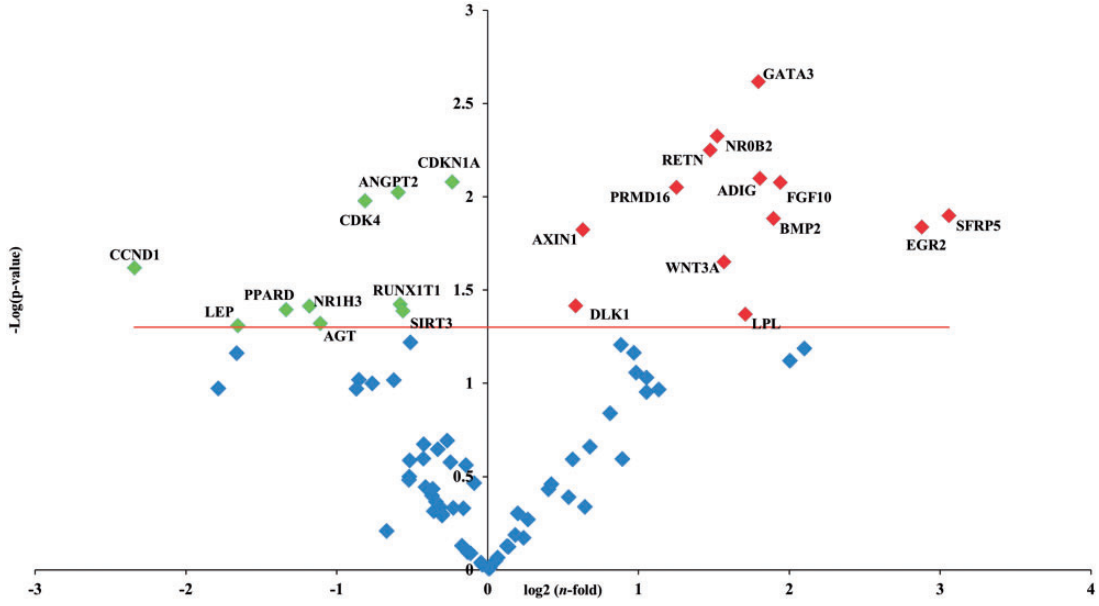

Figure 4 Volcano plot of adipogenesis PCR array. PCR array analysis of gene expression in RO-treated P20 cells in comparison to P20 CTRL cells. Total RNA was isolated from three independent experiments, one per each donor, were prepared for both CTRL and RO extract incubation. Cells were used at the third passage. The relative expression levels for each gene depicted as $\log_2$(*n*-fold) are plotted against -Log(p-value). Red indicator = significantly up-regulated gene; Green indicator = significantly down-regulated gene. Red line = indicates −Log(p value), $P < 0.05$. (A color version of this figure is available in the online journal.)

CEBPβ, CEBPδ, and PPARγ, although numerically lower in RO treated than CTRL cells, did not reach the threshold of significance (supplementary files Table 1). Conversely, genes with antiadipogenic effects, as GATA binding protein 3 (GATA3) and wingless-type MMTV integration site family, member 3A (WNT3A), were significantly ($P < 0.05$) up-regulated.

Differentially expressed miRNAs and validated target genes

Twenty-three significantly differentially expressed miRNAs between RO treated and CTRL P20 cells were identified (Table 2). Considering the role of miRNAs in the post-transcriptional control, the identification of validated target genes of differentially expressed miRNAs was studied by

Table 2 Different expression of miRNAs between RO-treated P20 preadipocytes and CTRL P20 preadipocytes. Data are expressed as the mean of miRNA mean transcript ± SD

	miRNA	P20-CTRL ± SD	P20-RO ± SD	*P* value
Down-regulated	miR-503	1.350 ± 0.050	0.000 ± 0.000	0.000
	miR-501	1.690 ± 0.100	0.000 ± 0.000	0.000
	miR-331	1.370 ± 0.140	0.000 ± 0.000	0.000
	miR-181a-1	4.470 ± 0.090	0.630 ± 0.010	0.000
	miR-143	2.710 ± 0.050	0.920 ± 0.010	0.000
	miR-99b	2.730 ± 0.040	1.200 ± 0.070	0.000
	miR-127	9.520 ± 1.350	2.080 ± 0.180	0.000
	miR-30a	3.630 ± 0.890	0.000 ± 0.000	0.001
	miR-181b-1	3.720 ± 0.800	0.670 ± 0.000	0.001
	miR-140	8.390 ± 1.500	4.170 ± 0.440	0.005
	miR-17	13.020 ± 1.700	8.460 ± 1.200	0.019
	miR-152	3.710 ± 0.210	2.850 ± 0.450	0.020
Up-regulated	miR-500b	0.000 ± 0.000	1.310 ± 0.090	0.000
	miR-378a	0.000 ± 0.000	1.390 ± 0.050	0.000
	miR-98	0.000 ± 0.000	1.560 ± 0.300	0.000
	miR-138-1	0.000 ± 0.000	2.300 ± 0.370	0.000
	miR-33b	1.950 ± 0.050	4.240 ± 0.340	0.000
	miR-296	0.000 ± 0.000	0.980 ± 0.350	0.004
	miR-let7f-1	2.460 ± 0.220	3.580 ± 0.560	0.016
	miR-365b	12.560 ± 0.140	29.630 ± 6.740	0.017
	miR-708	1.610 ± 0.210	2.200 ± 0.300	0.025
	miR-3913-1	1.360 ± 0.020	2.320 ± 0.480	0.032
	miR-193a	4.950 ± 0.800	6.810 ± 0.730	0.041

using miRWalk tool. To use the correct nomenclature, miRNA accession numbers were obtained by miRBase database.[46]

One thousand two hundred and thirty target genes were obtained corresponding to 21 differentially expressed miRNAs (supplementary files Table 2), apart from miR-501, miR-500b, and miR-3913-1, which were not found in the database of validated gene target. The total number of target genes from down-regulated miRNAs was 980, that from up-regulated 447, shared target genes were 197. The VENNY tool analysis was applied using the 1230 validated genes target, the 2415 validated genes of miRNAs-adipocyte (namely here ''Adipocytes'') and the 23 significantly differentially expressed genes obtained by PCR array. Genes shared from the three lists were 13 and specifically: CCND1, CDKN1A, lipoprotein lipase (LPL), bone morphogenetic protein 2 [BMP2], CDK4, GATA3, early growth response 2 (EGR2), angiotensinogen [AGT], runt-related transcription factor 1 (RUNX1T1), angiopoietin 2 [ANGPT2], delta-like 1 homolog (Drosophila) (DLK1), nuclear receptor subfamily 0, group B, member 2 (NR0B2), WNT3A. Five genes were common to ''miRNA-Seq,'' ''PCR Array,'' and ''Adipocytes'' (CCND1, CDKN1A, CDK4, LPL, BMP2); four genes were common to ''PCR Array'' and ''Adipocytes'' (GATA3, EGR2, AGT, RUNX1T1); and four genes common to ''miRNA-Seq'' and ''PCR Array'' (DLK1, NR0B2, ANGPT2, WNT3A). The Venny diagram and shared genes with their regulation are shown in Figure 5.

Analysis of the signaling pathways and biological process

Although the results of pathway enrichment analysis, provided by KEGG, showed that the most significant pathways, affected by 769 target genes of down and up-regulated miRNAs, were mainly involved in different types of cancer, we reported: ''cell cycle'' affected by 97 target genes of nine down-regulated, three up-regulated miRNAs; ''p53 signaling pathway'' affected by 73 target genes of eight down-regulated, four up-regulated miRNAs; ''Jak-STAT signaling pathway'' affected by 78 target genes of seven down-regulated, four up-regulated miRNAs; ''apoptosis'' affected by 69 of seven down-regulated, four up-regulated miRNAs; ''regulation of adipocytokine signaling pathway'' affected by 33 target genes of three down-regulated, three up-regulated miRNAs; and ''Wnt signaling pathway'' affected by 19 target genes of one down-regulated, three up-regulated miRNAs (supplementary files Table 3).

To further elucidate the possible roles of regulated microRNAs in the antiadipogenic RO-treated cells, GO enrichment for biological processes, cellular component, and molecular functions of regulated microRNA targets were performed. Table 3 presents the number of various biological themes significantly enriched for the targets of

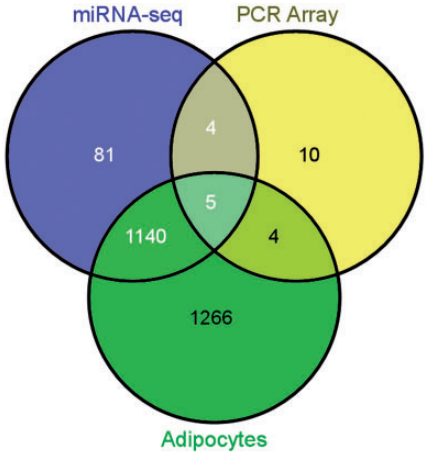

Shared genes	Regulation in this study
AGT	down
ANGPT2	down
CCND1	down
CDK4	down
CDKN1A	down
RUNX1T1	down
BMP2	up
DLK1	up
EGR2	up
GATA3	up
LPL	up
NR0B2	up
WNT3A	up

Figure 5 Venn diagram showing relation between validated genes target (1230 genes) of miRNA-seq significantly up- and down- regulated (miRNA-seq), validated genes of miRNAs-adipocyte (Adipocytes) (2415 genes) and significantly differentially expressed genes (23 genes) obtained by PCR array (PCR Array). Table shows the list of 13 shared genes and their regulation (as shown in Volcano plot) (A color version of this figure is available in the online journal.)

regulated miRNAs. In particular, the first 69 most significant biological processes, evaluated according to Bonferroni's correction, were controlled by down-regulated miR-17, miR-143, miR-181a, and miR-181b. ''Positive regulation of macromolecule metabolic process,'' ''regulation of cell proliferation,'' and ''regulation of cell death'' were significantly enriched for the target genes of miRNAs down-regulated in RO-treated P20 cells (supplementary files Table 4).

The results of pathway enrichment analysis provided by KEGG within $P < 0.05$ showed that the 13 shared genes, obtained by Venny analysis, are involved in seven pathways such as pathways in ''cancer,'' ''bladder cancer,'' ''glioma,'' ''p53 signaling pathway,'' ''melanoma,'' ''chronic myeloid leukemia,'' and ''cell cycle.'' Among them and in relation to adipose cell, ''cell cycle'' was more promising pathway to be affected by RO treatment.

GO enrichment analysis of shared genes for biological processes, cellular components, and molecular functions were also performed at $P < 0.05$. This analysis provided 62

Table 3 The number of various enriched biological themes (P value <0.05) for targets of differentially expressed miRNAs

Differentially expressed miRNAs		GO biological process ($P < 0.05$)	GO cellular component ($P < 0.05$)	GO-molecular function ($P < 0.05$)
Down-regulated	miR-503	161	9	19
	miR-331	145	13	25
	miR-181a-1	551	44	41
	miR-143	497	40	49
	miR-99b	188	9	11
	miR-127	215	10	11
	miR-30a	403	69	51
	miR-181b-1	519	43	40
	miR-140	381	27	31
	miR-17	748	45	59
	miR-152	223	17	16
Up-regulated	miR-378a	143	13	23
	miR-98	407	16	10
	miR-138-1	132	8	16
	miR-33b	96	13	11
	miR-296	342	16	32
	miR-let7f-1	782	37	70
	miR-365b	260	9	7
	miR-708	55	0	6
	miR-193a	353	8	10

biological processes, four cellular components, and five molecular processes. Among the various biological themes significantly enriched, ''G1/S transition of mitotic cell cycle,'' ''regulation of cell cycle,'' ''regulation of cell proliferation,'' ''fat cell differentiation,'' and ''regulation of cyclin-dependent protein kinase activity'' were the most interesting. The most significant molecular function was ''cyclin-dependent protein kinase regulator activity.'' Interestingly, the first 10 biological processes of down-regulated genes significantly enriched were: ''positive regulation of fibroblast proliferation,'' ''regulation of fibroblast proliferation,'' ''G1/S transition of mitotic cell cycle,'' ''positive regulation of cell proliferation,'' ''interphase of mitotic cell cycle,'' ''interphase,'' ''regulation of cell proliferation,'' and ''regulation of cell size.''

Discussion

Several studies reported that plant extracts and their bioactive components may have effects on adipose tissue.[11,13] The RO extracts contain natural antioxidants with reported applications for a wide range of health conditions such as cancer, cardiovascular disease, diabetes, and obesity.[47–49] RO has been shown to reduce blood glucose and cholesterol levels and also weight gain in mice fed with high-fat diet.[50] Glucose consumption has been demonstrated to increase in HepG2 cells treated with RO extract by activating AMPK pathway and regulating genes involved in metabolism such as sirtuin 1.[51]

Published evidences showed the inhibitory effect of carnosic acid, a bioactive component of RO, on differentiation in 3T3-L1 murine cells.[19,20] Clonal cell lines are homogenous in terms of cellular population since they are all at the

same differentiation stage, allowing a homogeneous response to treatments.[52] However, species-related differences in adipose tissue biology are known and also cell line-related artifacts have to be considered.[53] Therefore, to reproduce with higher fidelity the possible effects of RO extract, primary human adipocytes were used as model. Moreover, visceral adipose tissue adipocytes were chosen as target of RO activity, since they are more metabolically active, more sensitive to lipolysis, and more insulin resistant than subcutaneous adipocytes.[54] To elucidate the influence of RO extract on human primary omental preadipocytes, the accumulation of triglyceride was investigated during differentiation. Results with 30 μg/mL of RO extract indicated an inhibition of triglyceride incorporation in human visceral preadipocytes. Interestingly, the reduction of triglyceride incorporation during differentiation was coincident with an enhancement of lipolytic activity, as detected by an increase of glycerol release, in RO treated-P20 adipocytes and A7 adipocytes (Figures 2 and 3).

To better find out the potential antiadipogenic effect of RO, the expression pattern of adipogenesis-related genes was investigated on differentiating preadipocytes (P20) treated with RO extract and compared to control preadipocytes (Figure 4 and SM Table 1). CCND1, WNT3A, and GATA3 were found by the screening of miRNAs target genes. These genes are involved in Wnt signaling and cell cycle regulation. Accordingly, it has been shown that constitutive expression of GATA3 determined protein/protein interactions with CEBPα leading to the down-regulation of PPARγ and following repressed adipocyte differentiation in preadipocyte 3T3-L1 cells.[55] GATA3 is known to block cells at the preadipocyte stage, probably binding PPARγ promoter thus preventing its transcription.[56] Master regulators of adipocyte life, CEBPα and PPARγ, were down-expressed in RO-treated P20 cell, even though not significantly. Their weak modulation could be due to the use of visceral human preadipocytes, since PPARγ activity is noticeably lower in primary human visceral adipocytes than subcutaneous adipocytes.[53,57]

In a recent paper,[58] during 3T3-L1 differentiation, GATA3 was negatively regulated by miR-183 through the inhibition of the canonical Wnt/β-catenin signaling pathway, hence leading to adipogenic differentiation and adipogenesis. Although miR-183 was not listed in miRNAs-seq significant data (Table 2), GATA3 and WNT3A, known as inhibitors of preadipocyte to adipocyte transition, were the significantly ($P < 0.001$) highest expressed genes. Notably, ample evidences reported that Wnt signaling has a role in preventing adipocyte differentiation.[59,60] Specifically, Wnt canonical pathway activation blocks adipogenic conversion of 3T3-L1 preadipocytes through stabilization of β-catenin and inhibition of CEBPα and PPARγ.[61] It has been shown that WNT3A led to a dedifferentiation also of human adipocytes.[62,63] On the contrary, in absence of Wnt signaling activation, cytoplasmic β-catenin is recruited to a degradation complex, mediated by Axin, that facilitates its sequential phosphorylation by casein kinase I and glycogen synthase kinase 3β (GSK3β), provoking ubiquitination and proteasomal degradation of β-catenin.[59] Actually from PCR adipogenesis array data, some genes involved in up- and downstream Wnt signaling were significantly over-expressed as WNT3A, secreted frizzled-related protein 5, axin 1 (AXIN1) and others down-regulated as Dickkopf WNT signaling pathway inhibitor 1 (DKK1), CCND1, CDKN1A, and CDK4. The secreted protein DKK1 was found to be the most efficient inhibitor of canonical Wnt signaling binding Lrp5/6.[64] The down-regulation of DKK1 in RO-treated P20 cells could accomplish the over-expression of WNT3A. Moreover, other studies suggested that the canonical ligand WNT3A inhibited mutual activation of PPARγ and CEBPα in order to elicit its antiadipogenic effects.[65]

To clarify the involvement of Wnt signaling and of cyclin-dependent regulatory activity, as observed by GO functional annotation analysis, attention was paid to the miRNAs expression (Table 2). In 3T3-L1 preadipocytes, treated with an inhibitor of GSK3β to activate Wnt signaling, and compared to preadipocytes normally differentiated, miR-503 was strongly down-regulated.[66] Moreover, miR-30a was also down-regulated in the same cells in comparison to preadipocytes treated for a suppression of Wnt signaling.[66] In agreement with these observations, RO-treated P20 cells showed a shortage in both miRNAs ($P < 0.001$), suggesting an activation of Wnt signaling. However, targets of miR-503 were CCND1 and WNT3A that were oppositely modulated in RO-treated P20 cells. In this way, a possible activation of Wnt signaling by WNT3A over-expression did not correspond to a stimulation of β-catenin, which activates target genes involved in cell cycle such as CCND1. D-type cyclins and the cyclin-dependent kinases 4 and 6 act in early G1 phase in response to external stimuli during MCE required in the 3T3-L1 differentiation.[60,67] Additionally, CDK4 gene, target of CCND1, was down-expressed in RO-treated P20 cells. Moreover, CDK4 controlled also the activity of PPARγ through E2F activation during MCE.[67] However, present data do not support these observations since PPARγ and the effector of cyclin/cdk pathway in cell cycle regulation E2F transcription factor 1 (E2F1) did not significantly change. Notably, carnosic acid, active compound of RO, was demonstrated to induce cell cycle arrest predominantly at G2/M phase in human cancer cell lines altering cyclins level.[68,69]

However, it should be also noted that AXIN1, which participates in degradation of β-catenin through the activity of the axin complex, was significantly over-expressed in P20-treated cells (Figure 4; SM Table 1). Hence, from present data, although the activation of Wnt signaling could be suggested, the expression of downstream genes would indicate a repression of cell cycle and proliferation.

Let-7 is known to present numerous isoforms that decreased from day 0 to day 1 of differentiation and then increased till day 6 in 3T3-L1 cells and this was congruous with an impaired clonal expansion.[70] Let-7 transfection induced cell cycle delay through a down-regulation of several cell cycle genes (CCND1, CDK4) in 3T3-L1 cells.[70] This is consistent with results obtained from RO-treated cells that showed a significant expression of let-7f-1, which was up-regulated 1.45-fold in comparison to control cells (Table 2). Moreover, miRNA let-7f has been recognized as a key factor targeting the stabilization of axin 2, which promotes

β-catenin degradation in hMSC cells.[71] Let-7 has also a role in regulating the baseline expression of β2-adrenergic receptors, which are known to be involved in lipolytic pathway.[72] In fact in P20-treated cells, lipolysis increased and adrenoceptor beta 2 mRNA was not significantly affected ($\log_2[n\text{-fold}] = 0.89$, $P = 0.25$) (supplementary files Table 1).

miR-143 are normally up-regulated in mouse preadipocytes and it accelerates the rate of fat cell formation when expressed ectopically in 3T3-L1.[32,33] It is known that miR-143 promotes adipocyte differentiation by directly targeting mitogen-activated protein kinase 5 mRNA in rats inguinal ADSCs cells,[73] thereby inducing the transition from clonal expansion to terminal differentiation.[58] Based on the regulation theory that indicated miRNAs as molecules causing translation repression or the cleavage of the target mRNAs, the significant down-regulation of miR-143 in RO-treated P20 cells could have induced the inhibition of adipocyte terminal differentiation (Table 2).

Moreover, in hAD-MSC cells the overexpression of miR-138 was demonstrated to reduce lipid droplets accumulation, to inhibit expression of key adipogenic transcription factors CEBPα and PPARγ2 as well as several molecules associated with lipid metabolism, such as fatty acid binding protein 4, adipocyte (FABP4), and LPL.[74] In RO-treated P20 cells, miR-138 was up-regulated up twofold (Table 2; $P < 0.001$), but did not cause a significant under-expression of FABP4 ($\log2[n\text{-fold}] = -0.17$, $P = 0.74$), CEBPα ($\log_2[n\text{-fold}] = -0.67$, $P = 0.62$) and PPARγ ($\log_2[n\text{-fold}] = -0.032$, $P = 0.94$) (supplementary files Table 1).

Among miRNAs involved in adipogenesis regulation, miR-181a were down-expressed in RO-treated cells and this is in agreement with results achieved in subcutaneous fat tissue of seven-day-old piglets.[75] In those cells, the suppression of miR-181a led to inhibition of adipocyte differentiation by affecting the expression of tumor necrosis factor-α, as well as genes involved in adipogenesis.[75] In 3T3-L1 cells, miR-181a was also included among miRNAs that target transcription factors or differentiation markers during adipogenesis and that activate Wnt signaling.[66]

Although miR-130 has been recognized to have an anti-adipogenic function through direct regulation of PPARγ expression in human primary adipocytes,[76] it was not significantly listed in miRNAs-seq data (Table 2).

To further elucidate the results of up- and down-regulated miRNAs obtained by RNA-seq analysis, KEGG analysis was performed. The results indicated a regulation of cell cycle, apoptosis, and to a minor extent, Wnt signaling pathway (supplementary files Table 3). Most of the GO biological processes and molecular function (Table 3; $P < 0.05$ and supplementary files Table 4) were associated to the down-regulated miR-17, which is known to accelerate adipocyte differentiation by negatively regulating tumor suppressor Rb2/p130 (retinoblastoma-like 2)[77] and E2F1 regulation.[78]

Conclusions

In conclusion present study has two main strengths. The first was the use of standardized extract to define a protocol to study the bioactivity of nutraceuticals on cell functions and molecular targets. The second was the effort to investigate the possible effects on primary human visceral preadipocytes considering their unique role in the pathogenesis of the metabolic syndrome.

Noteworthy, this study has some limitations. The number of subjects was relatively small and the described associations between gene expression and miRNA-seq data will require confirmation in larger cohorts.

Times and types of miRNAs involved in adipocytes function and development often differed from the signaling events well known in 3T3-L1. However, let-7f-1, miR-17, miR-503, and miR-30a were particularly interesting since their role in modulating genes involved in cell cycle.

As first approach, this study showed the possibility of RO extract to modulate the adipocyte life cycle at different levels in part through a newly defined mechanism, i.e. the miRNAs cascade.

Authors' contributions: BS was the supervisor; EP was responsible for cellular experiments; MC was the originator and participated in analytical work, ran a majority of the statistics, and wrote the manuscript.

ACKNOWLEDGEMENTS

This work was supported by Progetto ART. 13 D.LGS 297/99, Italy.

REFERENCES

1. Kelly T, Yang W, Chen CS, Reynolds K, He J. Global burden of obesity in 2005 and projections to 2030. *Int J Obes* 2008;**32**:1431–7
2. Jialal I, Kaur H, Devaraj S. Toll-like receptor status in obesity and metabolic syndrome: a translational perspective. *J Clin Endocrinol Metab* 2014;**99**:39–48
3. Gray SL, Vidal-Puig AJ. Adipose tissue expandability in the maintenance of metabolic homeostasis. *Nutr Rev* 2007;**65**:S7–S12
4. Kwon H, Pessin JE. Adipokines mediate inflammation and insulin resistance. *Front Endocrinol (Lausanne)* 2013;**4**:71–84
5. Hajer GR, van Haeften TW, Visseren FL. Adipose tissue dysfunction in obesity, diabetes, and vascular diseases. *Eur Heart J* 2008;**29**:2959–71
6. Singla P, Bardoloi A, Parkash AA. Metabolic effects of obesity: a review. *World J Diabetes* 2010;**1**:76–88
7. Crujeiras AB, Díaz-Lagares A, Carreira MC, Amil M, Casanueva FF. Oxidative stress associated to dysfunctional adipose tissue: a potential link between obesity, type 2 diabetes mellitus and breast cancer. *Free Radic Res* 2013;**47**:243–56
8. Rosen ED, MacDougald OA. Adipocyte differentiation from the inside out. *Nat Rev Mol Cell Biol* 2006;**7**:885–96
9. Waxman A. World Health Assembly. WHO global strategy on diet, physical activity and health. *Food Nutr Bull* 2004;**25**:292–302
10. Billon N, Dani C. Developmental origins of the adipocyte lineage: new insights from genetics and genomics studies. *Stem Cell Rev* 2012;**8**:55–66
11. Colitti M, Grasso S. Nutraceuticals and regulation of adipocyte life: premises or promises. *Biofactors.* Epub ahead of print 2 April 2014. DOI 10.1002/biof.1164
12. González-Castejón M, Rodriguez-Casado A. Dietary phytochemicals and their potential effects on obesity: a review. *Pharmacol Res* 2011;**64**:438–55
13. Rayalam S, Della-Fera MA, Baile CA. Phytochemicals and regulation of the adipocyte life cycle. *J Nutr Biochem* 2008;**19**:717–26
14. Yun JW. Possible anti-obesity therapeutics from nature–a review. *Phytochem* 2010;**71**:1625–41
15. Bravo L. Polyphenols: chemistry, dietary sources, metabolism, and nutritional significance. *Nutr Rev* 1998;**56**:317–33

16. Al-Sereiti MR, Abu-Amer KM, Sen P. Pharmacology of rosemary (*Rosmarinus officinalis* Linn.) and its therapeutic potentials. *Indian J Exp Biol* 1999;**37**:124–30
17. Luqman S, Dwivedi GR, Darokar MP, Kalra A, Khanuja SP. Potential of rosemary oil to be used in drug-resistant infections. *Altern Ther Health Med* 2007;**13**:54–59
18. Harach T, Aprikian O, Monnard I, Moulin J, Membrez M, Béolor JC, Raab T, Macé K, Darimont C. Rosemary (*Rosmarinus officinalis* L.) leaf extract limits weight gain and liver steatosis in mice fed a high-fat diet. *Planta Med* 2010;**76**:566–71
19. Takahashi T, Tabuchi T, Tamaki Y, Kosaka K, Takikawa Y, Satoh T. Carnosic acid and carnosol inhibit adipocyte differentiation in mouse 3T3-L1 cells through induction of phase2 enzymes and activation of glutathione metabolism. *Biochem Biophys Res Commun* 2009;**382**:549–54
20. Gaya M, Repetto V, Toneatto J, Anesini C, Piwien-Pilipuk G, Moreno S. Antiadipogenic effect of carnosic acid, a natural compound present in *Rosmarinus officinalis*, is exerted through the C/EBPs and PPARγ pathways at the onset of the differentiation program. *Biochim Biophys Acta* 2013;**830**:3796–806
21. Ninomiya K, Matsuda H, Shimoda H, Nishida N, Kasajima N, Yoshino T, Morikawa T, Yoshikawa M. Carnosic acid, a new class of lipid absorption inhibitor from sage. *Bioorg Med Chem Lett* 2004;**14**:1943–6
22. Fu Y, Luo N, Klein RL, Garvey WT. Adiponectin promotes adipocyte differentiation, insulin sensitivity, and lipid accumulation. *J Lipid Res* 2005;**46**:1369–79
23. Tsai M, Asakawa A, Amitani H, Inui A. Stimulation of leptin secretion by insulin. *Indian J Endocrinol Metab* 2012;**16**:S543–8
24. Ntambi JM, Young-Cheul K. Adipocyte differentiation and gene expression. *J Nutr* 2000;**130**:3122S–6S
25. Ross SE, Hemati N, Longo KA, Bennett CN, Lucas PC, Erickson RL, MacDougald OA. Inhibition of adipogenesis by Wnt signalling. *Science* 2000;**289**:950–3
26. Prokesch A, Hackl H, Hakim-Weber R, Bornstein SR, Trajanoski Z. Novel insights into adipogenesis from omics data. *Curr Med Chem* 2009;**16**:2952–64
27. Dhar S, Hicks C, Levenson AS. Resveratrol and prostate cancer: promising role for microRNAs. *Mol Nutr Food Res* 2011;**55**:1219–29
28. Gandhy SU, Kim K, Larsen L, Rosengren RJ, Safe S. Curcumin and synthetic analogs induce reactive oxygen species and decreases specificity protein (Sp) transcription factors by targeting microRNAs. *BMC Cancer* 2012;**12**:564
29. Kumazaki M, Noguchi S, Yasui Y, Iwasaki J, Shinohara H, Yamada N, Akao Y. Anti-cancer effects of naturally occurring compounds through modulation of signal transduction and miRNA expression in human colon cancer cells. *J Nutr Biochem* 2013;**24**:1849–58
30. Peng Y, Yu S, Li H, Xiang H, Peng J, Jiang S. MicroRNAs: emerging roles in adipogenesis and obesity. *Cell Signal* 2014;**26**:1888–96
31. McGregor RA, Choi MS. microRNAs in the regulation of adipogenesis and obesity. *Curr Mol Med* 2011;**11**:304–16
32. Romao JM, Jin W, Dodson MV, Hausman GJ, Moore SS, Guan LL. MicroRNA regulation in mammalian adipogenesis. *Exp Biol Med (Maywood)* 2011;**236**:997–1004
33. Xie H, Lim B, Lodish HF. MicroRNAs induced during adipogenesis that accelerate fat cell development are downregulated in obesity. *Diabetes* 2009;**58**:1050–7
34. Yu J, Kong X, Liu J, Lv Y, Sheng Y, Lv S, Di W, Wang C, Zhang F, Ding G. Expression profiling of PPARγ-regulated microRNAs in human subcutaneous and visceral adipogenesis in both genders. *Endocrinol* 2014;**155**:2155–65
35. Jeon TI, Park JW, Ahn J, Jung CH, Ha TY. Fisetin protects against hepatosteatosis in mice by inhibiting miR-378. *Mol Nutr Food Res* 2013;**57**:1931–7
36. Matoušková P, Bártíková H, Boušová I, Hanušová V, Szotáková B, Skálová L. Reference genes for real-time PCR quantification of messenger RNAs and microRNAs in mouse model of obesity. *PLoS One* 2014;**9**:e86033
37. Pomari E, Stefanon B, Colitti M. Effect of *Arctium lappa* (burdock) extract on canine dermal fibroblasts. *Vet Immunol Immunopathol* 2013;**156**:159–66
38. Bustin SA, Benes V, Garson JA, Hellemans J, Huggett J, Kubista M, Mueller R, Nolan T, Pfaffl MW, Shipley GL, Vandesompele J, Wittwer CT. The MIQE guidelines: minimum information for publication of quantitative real-time PCR experiments. *Clin Chem* 2009;**55**:611–22
39. Livak KJ, Schmittgen TD. Analysis of relative gene expression data using real-time quantitative PCR and the $2^{-\Delta\Delta Ct}$ method. *Methods* 2001;**25**:402–8
40. Anders S, McCarthy DJ, Chen Y, Okoniewski M, Smyth GK, Huber W, Robinson MD. Count-based differential expression analysis of RNA sequencing data using R and bioconductor. *Nat Protoc* 2013;**8**:1765–86
41. Robinson MD, McCarthy DJ, Smyth GK. edgeR: a Bioconductor package for differential expression analysis of digital gene expression data. *Bioinformatics* 2010;**26**:139–40
42. Dweep H, Sticht C, Pandey P, Gretz N. miRWalk-database: prediction of possible miRNA binding sites by ''walking'' the genes of three genomes. *J Biomed Inform* 2011;**44**:839–47
43. Oliveros JC. VENNY. *An interactive tool for comparing lists with Venn Diagrams,* http://bioinfogp.cnb.csic.es/tools/venny/index.html (2007, accessed)
44. Huang DW, Lempicki RA. Systematic and integrative analysis of large gene lists using DAVID bioinformatics resources. *Nat Protoc* 2009;**4**:44–57
45. SPSS® Statistical Package for Social Science SPSS. *Advanced Statistics 7.5*. Chicago, IL: SPSS Inc, 1997
46. Kozomara A, Griffiths-Jones S. miRBase: annotating high confidence microRNAs using deep sequencing data. *Nucleic Acids Res* 2014;**42**:D68–73
47. Hsieh CL, Peng CH, Chyau CC, Lin YC, Wang HE, Peng RY. Low-density lipoprotein, collagen, and thrombin models reveal that *Rosemarinus officinalis* L. exhibits potent antiglycative effects. *J Agric Food Chem* 2007;**55**:2884–91
48. Rau O, Wurglics M, Dingermann T, Abdel-Tawab M, Schubert-Zsilavecz M. Screening of herbal extracts for activation of the human peroxisome proliferator-activated receptor. *Pharmazie* 2006;**61**:952–6
49. Sinkovic A, Suran D, Lokar L, Fliser E, Skerget M, Novak Z, Knez Z. Rosemary extracts improve flow-mediated dilatation of the brachial artery and plasma PAI-1 activity in healthy young volunteers. *Phytother Res* 2011;**25**:402–7
50. Ibarra A, Cases J, Roller M, Chiralt-Boix A, Coussaert A, Ripoll C. Carnosic acid-rich rosemary (*Rosmarinus officinalis* L.) leaf extract limits weight gain and improves cholesterol levels and glycaemia in mice on a high-fat diet. *Br J Nutr* 2011;**106**:1182–9
51. Tu Z, Moss-Pierce T, Ford P, Jiang TA. Rosemary (*Rosmarinus officinalis* L.) extract regulates glucose and lipid metabolism by activating AMPK and PPAR pathways in HepG2 cells. *J Agric Food Chem* 2013;**61**:2803–10
52. Moreno-Navarrete JM, Fernández-Real JM. Adipocyte differentiation. In: Symonds ME (ed) *Adipose tissue biology*. Springer, New York, 2012, pp.17–38
53. Söhle J, Machuy N, Smailbegovic E, Holtzmann U, Grönniger E, Wenck H, Stäb F, Winnefeld M. Identification of new genes involved in human adipogenesis and fat storage. *PLoS One* 2012;**7**:e31193
54. Ibrahim MM. Subcutaneous and visceral adipose tissue: structural and functional differences. *Obes Rev* 2010;**11**:11–18
55. Hu Y, Davies GE. Berberine increases expression of GATA-2 and GATA-3 during inhibition of adipocyte differentiation. *Phytomedicine* 2009;**16**:864–73
56. Tong Q, Tsai J, Tan G, Dalgin G, Hotamisligil GS. Interaction between GATA and the C/EBP family of transcription factors is critical in GATA-mediated suppression of adipocyte differentiation. *Mol Cell Biol* 2005;**25**:706–15
57. Sauma L, Franck N, Paulsson JF, Westermark GT, Kjølhede P, Strålfors P, Söderström M, Nystrom FH. Peroxisome proliferator activated receptor gamma activity is low in mature primary human visceral adipocytes. *Diabetologia* 2007;**50**:195–201

58. Chen L, Hou J, Ye L, Chen Y, Cui J, Tian W, Li C, Liu L. MicroRNA-143 regulates adipogenesis by modulating the MAP2K5-ERK5 signalling. *Sci Rep* 2014;**4**:3819–28
59. Christodoulides C, Lagathu C, Sethi JK, Vidal-Puig A. Adipogenesis and WNT signalling. *Trends Endocrinol Metab* 2009;**20**:16–24
60. Lefterova MI, Lazar MA. New developments in adipogenesis. *Trends Endocrinol Metab* 2009;**20**:107–14
61. Ross SE, Erickson RL, Gerin I, DeRose PM, Bajnok L, Longo KA, Misek DE, Kuick R, Hanash SM, Atkins KB, Andresen SM, Nebb HI, Madsen L, Kristiansen K, MacDougald OA. Microarray analyses during adipogenesis: understanding the effects of Wnt signalling on adipogenesis and the roles of liver X receptor alpha in adipocyte metabolism. *Mol Cell Biol* 2002;**22**:5989–99
62. Lu H, Ward MG, Adeola O, Ajuwon KM. Regulation of adipocyte differentiation and gene expression-crosstalk between TGFβ and wnt signalling pathways. *Mol Biol Rep* 2013;**40**:5237–45
63. Gustafson B, Smith U. Activation of canonical wingless-type MMTV integration site family (Wnt) signalling in mature adipocytes increases beta-catenin levels and leads to cell dedifferentiation and insulin resistance. *J Biol Chem* 2010;**285**:14031–41
64. Christodoulides C, Laudes M, Cawthorn WP, Schinner S, Soos M, O'Rahilly S, Sethi JK, Vidal-Puig A. The Wnt antagonist Dickkopf-1 and its receptors are coordinately regulated during early human adipogenesis. *J Cell Sci* 2006;**119**:2613–20
65. Kawai M, Mushiake S, Bessho K, Murakami M, Namba N, Kokubu C, Michigami T, Ozono K. Wnt/Lrp/beta-catenin signalling suppresses adipogenesis by inhibiting mutual activation of PPARgamma and C/EBPalpha. *Biochem Biophys Res Commun* 2007;**363**:276–82
66. Qin L, Chen Y, Niu Y, Chen W, Wang Q, Xiao S, Li A, Xie Y, Li J, Zhao X, He Z, Mo D. A deep investigation into the adipogenesis mechanism: profile of microRNAs regulating adipogenesis by modulating the canonical Wnt/beta-catenin signalling pathway. *BMC Genomics* 2010;**11**:320
67. Abella A, Dubus P, Malumbres M, Rane SG, Kiyokawa H, Sicard A, Vignon F, Langin D, Barbacid M, Fajas L. Cdk4 promotes adipogenesis through PPARgamma activation. *Cell Metab* 2005;**2**:239–49
68. Visanji JM, Thompson DG, Padfield PJ. Induction of G2/M phase cell cycle arrest by carnosol and carnosic acid is associated with alteration of cyclin A and cyclin B1 levels. *Cancer Lett* 2006;**237**:130–6
69. Yesil-Celiktas O, Sevimli C, Bedir E, Vardar-Sukan F. Inhibitory effects of rosemary extracts, carnosic acid and rosmarinic acid on the growth of various human cancer cell lines. *Plant Foods Hum Nutr* 2010;**65**:158–63
70. Sun T, Fu M, Bookout AL, Kliewer SA, Mangelsdorf DJ. MicroRNA let-7 regulates 3T3-L1 adipogenesis. *Mol Endocrinol* 2009;**23**:925–31
71. Egea V, Zahler S, Rieth N, Neth P, Popp T, Kehe K, Jochum M, Ries C. Tissue inhibitor of metalloproteinase-1 (TIMP-1) regulates mesenchymal stem cells through let-7f microRNA and Wnt/β-catenin signalling. *Proc Natl Acad Sci USA* 2012;**109**:E309–16
72. Wang WC, Juan AH, Panebra A, Liggett SB. MicroRNA let-7 establishes expression of beta2-adrenergic receptors and dynamically down-regulates agonist-promoted down-regulation. *Proc Natl Acad Sci USA* 2011;**108**:6246–51
73. Esau C, Kang X, Peralta E, Hanson E, Marcusson EG, Ravichandran LV, Sun Y, Koo S, Perera RJ, Jain R, Dean NM, Freier SM, Bennett CF, Lollo B, Griffey R. MicroRNA-143 regulates adipocyte differentiation. *J Biol Chem* 2004;**279**:52361–5
74. Yang Z, Bian C, Zhou H, Huang S, Wang S, Liao L, Zhao RC. MicroRNA hsa-miR-138 inhibits adipogenic differentiation of human adipose tissue-derived mesenchymal stem cells through adenovirus EID-1. *Stem Cells Dev* 2011;**20**:259–67
75. Li H, Chen X, Guan L, Qi Q, Shu G, Jiang Q, Yuan L, Xi Q, Zhang Y. MiRNA-181a regulates adipogenesis by targeting tumor necrosis factor-α (TNF-α) in the porcine model. *PLoS One* 2013;**8**:e71568
76. Lee EK, Lee MJ, Abdelmohsen K, Kim W, Kim MM, Srikantan S, Martindale JL, Hutchison ER, Kim HH, Marasa BS, Selimyan R, Egan JM, Smith SR, Fried SK, Gorospe M. miR-130 suppresses adipogenesis by inhibiting peroxisome proliferator-activated receptor gamma expression. *Mol Cell Biol* 2011;**31**:626–38
77. Wang Q, Li YC, Wang J, Kong J, Qi Y, Quigg RJ, Li X. miR-17-92 cluster accelerates adipocyte differentiation by negatively regulating tumor-suppressor Rb2/p130. *Proc Natl Acad Sci USA* 2008;**105**:2889–94
78. Pickering MT, Stadler BM, Kowalik TF. miR-17 and miR-20a temper an E2F1-induced G1 checkpoint to regulate cell cycle progression. *Oncogene* 2009;**28**:140–5

(Received August 25, 2014, Accepted October 12, 2014)